

# Quantum Transport and Classical Dynamics in Open Billiards

H. Ishio<sup>1</sup>

Received January 4, 1995; final May 26, 1995

---

We report numerical results of an investigation of quantum transport for a weakly opened integrable circle and chaotic stadium billiards with a pair of conducting leads. While the statistics of spacings of resonance energies commonly follow the Wigner (GOE)-like distribution, the electric conductance as a function of the Fermi wavenumber shows characteristic noisy fluctuations associated with a typical set of classical orbits unique for both billiards. The wavenumber autocorrelation for the conductance is stronger in the stadium than the circle billiard, which we show is related to the length spectrum of classical short orbits. We propose an explanation of these contrasts in terms of the effect of phase decoherence due to the underlying chaotic dynamics.

---

**KEY WORDS:** Quantum transport; open billiards; chaos; Ericson fluctuation; path-length spectrum.

## 1. INTRODUCTION

During the last decade, remarkable advances in semiconductor fabrication technology have brought challenging devices not only for electronic engineers, but for those who study fundamental physics (see, e.g., ref. 1). Both experimentally and theoretically, there has been a great deal of interest in the electronic and magnetic properties of such *mesoscopic* systems and as a result a number of new physical phenomena have been observed and predicted (see, e.g., ref. 2). Among them, one of the most interesting topics is *chaotic boundary scattering* in systems formed in high-mobility GaAs/AlGaAs heterostructures where the system size is less than the elastic mean free path of electrons. In such systems, the motion of two-dimensional (2D) noninteracting electrons confined by wall of arbitrary geometry

---

<sup>1</sup> Division of Natural Science, Osaka Kyoiku University, Osaka 582, Japan.

is *ballistic*, and the classical “billiard” model successfully explains experimental results of those systems.<sup>(3)</sup> In the ballistic regime, the shape of walls directly determines the motion of electrons colliding with them, and the nonlinear dynamics of the electrons plays an essential role in quantum transport through the microstructures (see, e.g., ref. 4 and references therein).

One of the prototypes of conservative chaotic systems is the “stadium billiard.”<sup>(5)</sup> It belongs to the class of  $K$  systems and its quantum mechanical study has had a great impact on the field of *quantum chaos*.<sup>(6)</sup> On the other hand, realistic systems are more or less open systems and it is highly desirable to examine the effect of chaotic scattering on quantum transport in open systems.<sup>2</sup> In this context, studies of its open version have recently begun in connection with mesoscopic physics.<sup>(4, 8–12)</sup>

In this paper, we report numerical results of a detailed analysis of electric conductance fluctuations as a function of the Fermi wavenumber for *weakly opened* billiards without magnetic field, and show that the integrability of systems has a surprising effect on ballistic quantum transport.

The paper is organized as follows. The classical equation of motion of electrons is numerically solved for integrable and chaotic open billiards in Section 2. In Section 3 we summarize our work on their quantum dynamics to see the differences in conductance fluctuations. In Section 4 we focus in more detail on the signature of chaos in quantum transport. The results of a computation using semiclassical theory are compared with those of the quantum calculation discussed in Section 3. The first half of Section 2 and Sections 3.1 and 3.2 are based on joint work with Prof. K. Nakamura<sup>(9)</sup> and the latter half of Section 2, Section 3.3, and Section 4 are a direct application of joint work with Prof. J. Burgdörfer<sup>(12)</sup> to the geometry of the model we adopt in this paper.

## 2. COMPUTATION OF CLASSICAL DYNAMICS

Figure 1 represents an open stadium characterized by  $a$ ,  $l$ , and  $d$  for the radius of a semicircle, the half-length of a line segment, and the width of holes at  $x = a_1$ ,  $a_2$ , respectively. We shall prescribe  $a_1 = -a'$  and  $a_2 = a'$ , with  $a' = l + (a^2 - d^2/4)^{1/2}$ . While the aspect ratio  $\sigma \equiv l/a$  will be tunable, the area of the billiard  $A (= \pi a^2 + 4al)$  will be kept fixed and all lengths will be scaled by  $\sqrt{A}$ . Here we shall concentrate on a weakly opened situation where the width of the holes is small in comparison with the dimension of the billiard and ample fluctuation properties are anticipated in

<sup>2</sup> For review of quantum chaotic scattering see, e.g., refs. 7.

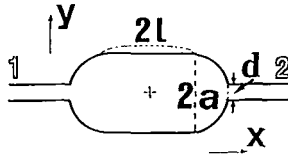


Fig. 1. Schematic diagram for open stadium billiard. “+” is the origin of the  $(x, y)$  coordinates.

quantum transport. For convenience,  $d/\sqrt{A} = 0.0935$  will be chosen below. Edges of leads 1 and 2 are assumed to be located at the left and right holes, respectively. We shall call the region lying inside the billiard and satisfying  $|x| < a'$  the “cavity region.” Chaotic scattering of electrons in this region will control the conductance.

As for the closed version of stadium billiards, the  $K$  entropy (maximum Lyapunov exponent) vanishes at the integrable limit  $\sigma = 0$  and takes a maximum at  $\sigma = 1^{(15)}$ ; these circle and fully chaotic billiards are hereafter abbreviated as  $C$  and  $S$  billiards, respectively. For the open-system version of the  $S$  billiard, when we calculate the distribution of the dwell time  $\tau$  [or path length  $L$  ( $\propto \tau$ )] during which an incoming electron with a given

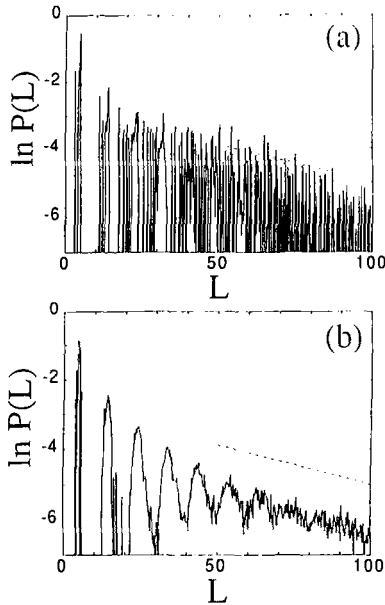


Fig. 2. Path-length spectrum  $P(L)$ : (a) circle; (b) stadium. Dashed line represents the exponential decay exponent  $\gamma$  ( $\approx 0.0223$ ) predicted by Jensen.<sup>(13)</sup>  $L$  is normalized as  $A = \pi + 4$ .

injection angle  $\theta_0$  at hole 1 dwells inside the cavity region, it exhibits a fine comblike structure consisting of multiple scales, resulting in nice self-similar or fractal structures.<sup>(9)</sup> For the *C* billiard, on the contrary, neither fine structures nor self-similarity can be perceived.

Figure 2 shows Monte Carlo simulations of the classical path-length spectrum for the open *C* and *S* billiards. The path-length spectrum  $P(L)$  has characteristic structures in addition to a cusp corresponding to the “direct” path connecting the leads 1 and 2. In case of the open *C* billiard, the function  $P(L)$  consists of a large number of cusps with narrow width, each of which corresponds to a bundle of trajectories for transmission (Fig. 2a). In the case of the open *S* billiard,  $P(L)$  displays a sequence of almost equidistant broad peaks in the short-length region  $L \lesssim 70$  (Fig. 2b). The period of these peaks corresponds approximately to the perimeter length of the cavity region. For longer path lengths in the open *S* billiard, the proliferation of orbits tends to average out this structure, resulting in a coarse-grained exponential distribution<sup>(13, 14)</sup>

$$P_0(L) = \gamma \exp(-\gamma L) \tag{1}$$

with a decay constant  $\gamma = 2d/A\pi = 0.0223$  (dashed line in Fig. 2). Equation (1) has been verified numerically in the limit of long orbits.<sup>(4, 10)</sup>

### 3. COMPUTATION OF QUANTUM DYNAMICS

#### 3.1. Numerical Solution of the Schrödinger Equation

To see the quantum analog of the classical issues, we shall solve the Schrödinger equation for open systems,  $-(\hbar^2/2\mu) \nabla^2 \Psi = (\hbar^2/2\mu) k_F^2 \Psi$ , where  $k_F$  is the Fermi wavenumber. Define the wavevector  $\mathbf{k} = (k_m, m\pi/d)$  in the leads, where  $k_m = (k_F^2 - (m\pi/d)^2)^{1/2}$  ( $m = 1, 2, \dots$ ). For a propagating wave with mode  $n$  ( $\leq N = [k_F d/\pi]$ ) incoming through lead 1, the solution  $\Psi$  inside the leads  $j$  ( $= 1, 2$ ) is

$$\Psi_{\text{out}}^{(j)}(x, y; n) = \delta_{j1} e^{ik_n(x-a_1)} \phi_n(y) + \sum_{m=1}^{\infty} S_{mn}^{(j)} e^{i(-)^j k_m(x-a_j)} \phi_m(y) \tag{2}$$

where  $\phi_m(y) = (2/d)^{1/2} \sin((m\pi/d)(y + d/2))$  with  $|y| \leq d/2$ . On the other hand, the solution inside the cavity region is given in the form

$$\Psi_{\text{in}}(x, y) = (2/d)^{1/2} \int_0^{2\pi} c_n(\theta) e^{ik_F(x \cos \theta + y \sin \theta)} d\theta \tag{3}$$

$\Psi_{\text{in}}$  should satisfy the Dirichlet boundary condition,  $\Psi_{\text{in}}(x, y) = 0$ , at the hard walls.  $\Psi_{\text{out}}^{(1,2)}$  and  $\Psi_{\text{in}}$  should match at the holes. The continuity and smoothness conditions are given respectively by

$$\Psi_{\text{out}}^{(j)}|_{x=a_j} = \Psi_{\text{in}}|_{x=a_j}, \quad (d/dx) \Psi_{\text{out}}^{(j)}|_{x=a_j} = (d/dx) \Psi_{\text{in}}|_{x=a_j}, \quad j = 1, 2$$

These three boundary conditions could be solved simultaneously to obtain  $\{c_n\}$  and  $\{S_{nm}^{(j)}\}$ . Then we can calculate the conductance as a function of  $\sigma$  and the Fermi energy [ $\varepsilon_F = (\hbar k_F)^2/2\mu$ ] of incoming electrons by the application of Landauer's formula<sup>(15)</sup>:  $G = \sum_{n=1}^N G^{(n)}$  with  $G^{(n)} = (2e^2/h) \sum_{1 \leq m \leq N} |t_{mn}|^2$ , where  $t_{mn} = (k_m/k_n)^{1/2} S_{nm}^{(2)}$ .

### 3.2. Conductance Fluctuations and Correlations

Figure 3 shows the conductance  $G$  as a function of  $k_F$  ( $k_F d/\pi \leq 4.8$ ). Note: New modes appear at  $k_F d/\pi = n$  with  $n = 1, 2, \dots$  and  $G$  and  $G^{(1)}$  are identical for  $k_F d/\pi \leq 2$ . For both billiards the conductance  $G$  commonly exhibits very noisy fluctuations. Nevertheless the conductance, when coarse-grained, exhibits short-period and small-amplitude oscillations around some plateau value for the  $C$  billiard, but long-period and large-amplitude smooth oscillations for the  $S$  billiard.<sup>(9)</sup>

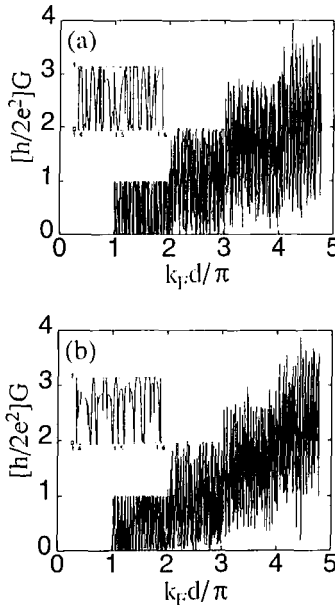


Fig. 3. Conductance  $G(k_F)$  for  $k_F d/\pi \leq 4.8$ : (a) circle; (b) stadium. Insets: Partial magnification for the range  $1.4 \leq k_F d/\pi \leq 1.6$ .

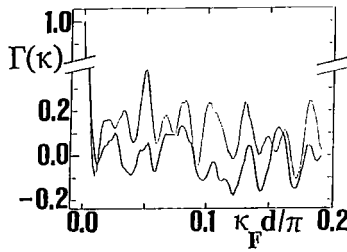


Fig. 4. Wavenumber autocorrelation function  $\Gamma(\kappa)$  for conductance  $G^{(1)}(k_F)$ . Solid and dotted lines correspond to open circle and stadium billiards, respectively. (From ref. 9.)

To characterize the fluctuations, we have calculated the wavenumber autocorrelation function

$$\Gamma(\kappa) \equiv \langle \delta G^{(1)}(k_F - \kappa/2) \delta G^{(1)}(k_F + \kappa/2) \rangle_{k_F} \quad (4)$$

with  $\delta G^{(1)} \equiv G^{(1)} - \langle G^{(1)} \rangle_{k_F}$ . In Fig. 4,  $\Gamma(\kappa)$  shows distinctive short-range behaviors<sup>(9)</sup>: (1) correlation as a whole is stronger in  $S$  than  $C$  billiards; (2) the central peak at the origin has almost the same width for both  $C$  and  $S$  billiards. The result (1) provides a logical foundation for the monotonic structure of the coarse-grained conductance for the  $S$  billiard. The result (2) indicates that both  $C$  and  $S$  billiards are commonly accompanied by Ericson-type fluctuations,<sup>(16)</sup> yielding an insight<sup>(17)</sup> into the relationship between fluctuations in random-matrix theory<sup>(18)</sup> and nonlinear dynamics.

The contrasts between  $C$  and  $S$  billiards prove to be more remarkable when  $d/\sqrt{A}$  is decreased. For a continuous change of  $\sigma$  from 0 through 1, conversion from short- to long-period and from small- to large-amplitude oscillations occurs.

### 3.3. Power Spectrum of Conductance Fluctuations

In order to quantify more precisely the suggestive difference in conductance oscillations discussed above, we have calculated the power spectrum of the conductance  $\delta G^{(1)}(k_F)$  (Fig. 5). (The results for the other modes have similar structures, though the strength of the peaks is a little different.) We can see prominent peaks at the positions  $L = 2.4, \dots$  for the  $C$  billiard and  $L = 0.5$  for the  $S$  billiard. These spectra correspond to the characteristic oscillations of the coarse-grained conductance for both billiards.

### 3.4. Statistics of Resonance Energies

The noisy conductance fluctuations as a function of  $k_F$  are a typical feature of weakly open systems, so long as poles of the  $S$ -matrix are well

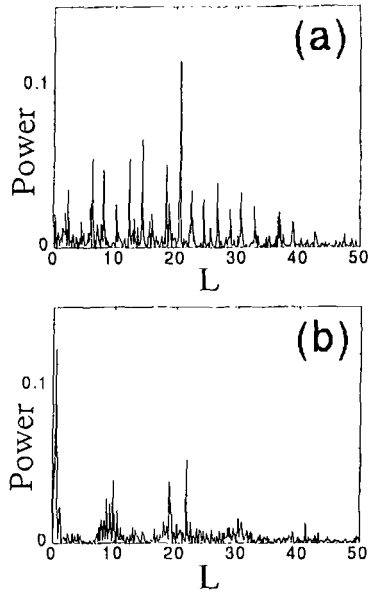


Fig. 5. Power spectrum of the conductance  $\delta G^{(1)}(k_F)$ : (a) circle; (b) stadium.  $L$  is normalized as  $A = \pi + 4$ .

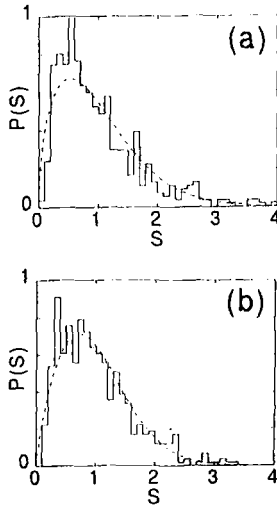


Fig. 6. Statistics of spacings of resonance energies in (a) open circle and (b) stadium billiards. The number of resonances is approximately 550 in both calculations. Dashed line represents a Brody distribution with a parameter (a)  $q = 0.5$  and (b)  $0.8$ .

concentrated. In our treatment both  $C$  and  $S$  billiards have the equal area  $A$  for their cavity region, ensuring almost equal concentration of poles. In both billiards, as shown in Fig. 6, the statistics of spacings of resonance energies follow the Wigner (GOE)-like distribution predicted by random-matrix theory.<sup>(18)</sup> When we approximate it with a Brody distribution

$$P_q(S) = \alpha S^q \exp(-\beta S^{1+q}) \quad (5)$$

the parameter  $q$  is roughly estimated as 0.5 and 0.8 for the  $C$  and  $S$  billiards, respectively. This implies that even a small perturbation or diffraction around the holes in an integrable open billiard immediately causes some nonintegrable effect on the statistics of resonances.<sup>(19)</sup>

## 4. SEMICLASSICAL ANALYSIS OF CONDUCTANCE FLUCTUATIONS

### 4.1. Fourier Spectrum of Scattering Amplitude and Classical Paths

In this section we explore the classical–quantum correspondence for conductance fluctuations in more detail. According to semiclassical theory,<sup>(20)</sup>

$$t_{mn} \sim \sum_s (D_{mn}^s)^{1/2} \exp\left(\frac{i}{h} \int_s \mathbf{p} \cdot d\mathbf{x} - i\pi \frac{\alpha_s}{2}\right) \quad (6)$$

where  $\alpha_s$  is the Maslov index,  $D_{mn}^s$  is the amplitude factor, and the sum is taken over all classical trajectories  $s$  connecting incoming channel  $n$  and outgoing channel  $m$ . The phase factor with the integral is rewritten as  $\exp(ik_F L_s)$  using the path length  $L_s$ .

When we evaluate the Fourier transform of the transmission amplitude  $t_{11}(k_F)$ , we find surprising features. In the case of the open  $C$  billiard, the spectrum in the region  $L \lesssim 42$  exhibits a sequence of prominent peaks which with a high accuracy correspond to a set of classical “asterisk” paths<sup>(12)</sup> connecting the entrance and exit in the cavity (Fig. 7a). On the other hand, in the case of the open  $S$  billiard, no evident peak appears other than the one which can be assigned to a simple path with single bouncing with strong regularity (Fig. 7b). In both cases, there exists a strong peak corresponding to a direct transmission without bouncing with a wall.



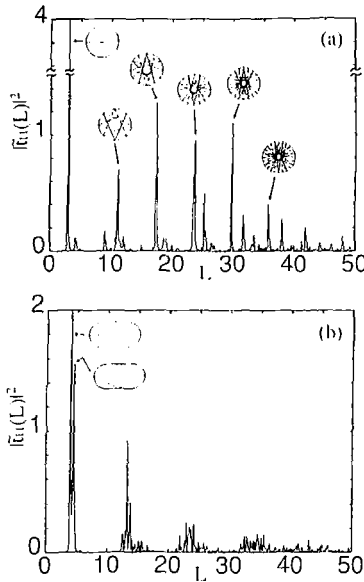


Fig. 7. Fourier spectrum of transmission amplitude  $t_{11}(k_F)$  and corresponding classical paths: (a) circle; (b) stadium.  $L$  is normalized as  $A = \pi + 4$ .

In the case of the open  $C$  billiard, each bundle of trajectories for transmission is separated enough and carrying a finite measure, which is an inherent property of an integrable system,<sup>3</sup> and this emphasizes the corresponding spectral peaks in  $\tilde{t}_{nm}$ . The almost equidistant peaks and the peak of direct transmission in the spectra  $\tilde{t}_{nm}$  for the open  $C$  billiard are related by Landauer's formula to the periods of conductance oscillations. There seems to be a selection rule that paths with smaller angles of incidence and transmittance survive in quantum transport, which suppresses all paths other than the asterisk paths. On the contrary, the insensitivity of the scattering matrix to  $k_F$  in the open  $S$  billiard reflects the stability of the classical ergodic phase space, as is discussed in refs. 9 and 11.<sup>4</sup> In Fig. 7b the two peaks at  $L = 4.00$  and  $4.47$ , which are remnants in the sea of chaos, cause the long-period oscillations observed in the coarse-grained conductance.<sup>(9)</sup>

<sup>3</sup> In open integrable systems, an incoming electron at entrance sees a "window" with finite measure for transmission into an exit, while in open chaotic systems, classical paths of electrons are mixed and intricate enough to produce infinitely small windows for transmission of each electron. See, e.g., dwell-time spectra shown in ref. 9.

<sup>4</sup> Analogous arguments were made for closed quantum billiards. See Nakamura and Thomas.<sup>(21)</sup>

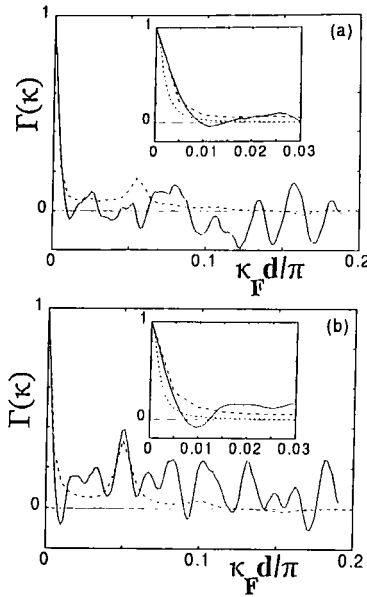


Fig. 8. Conductance autocorrelation function  $\Gamma(\kappa)$  (solid line) and Fourier transform of  $C(x)$  using  $P(L)$  averaged over the interval  $\Delta L = \pm 2$  (dashed line): (a) circle; (b) stadium. Insets: Partial magnification for  $\kappa d/\pi \leq 0.03$ . Dotted curve represents the Fourier transform of  $C(x) = P_0(x) \propto \exp(-\gamma x)$ , i.e., a Lorentzian  $1/[1 + (\kappa/\gamma)^2]$ .

## 4.2. Comparison of Correlation Functions with Semiclassical Results

In the previous section we showed the conductance autocorrelation function  $\Gamma(\kappa)$  obtained by a quantum calculation. In the semiclassical limit the Fourier transform of the classical length spectrum  $C(x) = \int_0^\infty P(L+x) P(L) dL$  gives the autocorrelation function  $\Gamma_{cl}(\kappa)$ .<sup>(4)</sup> Here  $P(L)$  is the path-length spectrum shown in Fig. 2.

Figure 8 shows that the quantum mechanical result of  $\Gamma(\kappa)$  and the Fourier transform of  $C(x)$  are in good agreement with each other. In the case of the open  $S$  billiard, the strong correlation at  $\kappa d/\pi \simeq 0.05$  in  $\Gamma(\kappa)$  is well reproduced by  $\Gamma_{cl}(\kappa)$  (Fig. 8b). The peak at  $\kappa d/\pi \simeq 0.05$  corresponds to the broad oscillations of  $P(L)$  with period  $L \simeq 10$  in Fig. 2b, and this period coincides approximately with the perimeter length of the stadium. Such oscillations of  $P(L)$  are clearly observed in the short-length region

( $L \lesssim 70$ ) and are smeared out for  $L \gtrsim 70$ , so that Eq. (1) is followed. The Fourier transform of  $P_0(L)$  gives a Lorentzian

$$\frac{\Gamma_0(\kappa)}{\Gamma_0(0)} = \frac{1}{1 + (\kappa/\gamma)^2} \quad (7)$$

and fits well to the cusp of  $\Gamma(\kappa)$  near  $\kappa = 0$  (insets of Fig. 8).<sup>(14)</sup>

## 5. CONCLUSIONS

In conclusion, from the viewpoint of the quantum mechanical manifestation of chaos, effects of chaotic scattering on quantum transport have been analyzed for weakly open integrable circle and fully chaotic stadium billiards with a pair of conducting leads. For both billiards, electric conductance as a function of Fermi wavenumber for each incident mode commonly shows very noisy fluctuations, and the statistics of spacings of resonance energies follow a Wigner (GOE)-like distribution. This implies that even a small perturbation around the holes immediately causes some nonintegrable effect on the statistics. Nevertheless wavenumber autocorrelation for the conductance is stronger in the stadium than the circle billiard. This contrast has been explained in terms of regular and chaotic orbits in the underlying classical dynamics. We have shown that the difference of the features in the autocorrelation functions comes from structures in the length spectra in the short-length regime accessible in experiments. In the Fourier spectrum of the quantum mechanical scattering amplitude, we can find traces of a set of classical paths in the integrable circle billiard.

## REFERENCES

1. M. A. Reed and W. P. Kirk, eds., *Nanostructure Physics and Fabrication* (Academic Press, New York, 1989).
2. B. L. Altshuler, P. A. Lee, and R. Webb, eds., *Mesoscopic Phenomena in Solids* (North-Holland, Amsterdam, 1991).
3. M. L. Roukes, A. Scherer, and B. P. Van der Gaag, *Phys. Rev. Lett.* **64**:1154 (1990); M. L. Roukes and O. L. Alerhand, *Phys. Rev. Lett.* **65**:1651 (1990); C. W. J. Beenakker and H. van Houten, in *Electronic Properties of Multilayers and Low-Dimensional Semiconductor Structures*, J. M. Chamberlain, L. Eaves, and J.-C. Portal, eds. (Plenum Press, New York, 1990), p. 75; C. W. J. Beenakker and H. van Houten, in *Solid State Physics*, Vol. 44, H. Ehrenreich and D. Turnbull, eds. (Academic Press, New York, 1991), p. 1.
4. H. U. Baranger, R. A. Jalabert, and A. D. Stone, *Chaos* **3**:665 (1993).
5. L. A. Bunimovich, *Funct. Anal. Appl.* **8**:254 (1974); G. Benettin and J. M. Strelcyn, *Phys. Rev. A* **17**:773 (1978).
6. S. W. McDonald and A. N. Kaufman, *Phys. Rev. Lett.* **42**:1189 (1979); E. J. Heller, *Phys. Rev. Lett.* **53**:1515 (1984).

7. M. C. Gutzwiller, *Chaos in Classical and Quantum Mechanics* (Springer, New York, 1990); U. Smilansky, in *Chaos and Quantum Physics*, M.-J. Giannoni, A. Voros, and J. Zinn-Justin, eds. (North-Holland, New York, 1991); K. Nakamura, *Quantum Chaos: A New Paradigm of Nonlinear Dynamics* (Cambridge University Press, Cambridge, 1993).
8. C. M. Marcus, A. J. Rimberg, R. M. Westervelt, P. F. Hopkins, and A. C. Gossard, *Phys. Rev. Lett.* **69**:506 (1992).
9. K. Nakamura and H. Ishio, *J. Phys. Soc. Jpn.* **61**:3939 (1992).
10. W. A. Lin, J. B. Delos, and R. V. Jensen, *Chaos* **3**:655 (1993).
11. K. Nakamura, K. Ito, and Y. Takane, *J. Phys. A* **27**:5889 (1994).
12. H. Ishio and J. Burgdörfer, *Phys. Rev. B* **51**:2013 (1995).
13. R. V. Jensen, *Chaos* **1**:101 (1991).
14. R. Blümel and U. Smilansky, *Phys. Rev. Lett.* **60**:477 (1988).
15. R. Landauer, *IBM J. Res. Dev.* **1**:223 (1957).
16. T. Ericson and T. Mayer-Kuckuk, *Annu. Rev. Nucl. Sci.* **16**:183 (1966).
17. E. Doron, U. Smilansky, and A. Frenkel, *Physica D* **50**:367 (1991).
18. M. L. Mehta, *Random Matrices*, 2nd ed. (Academic Press, New York, 1990).
19. H. Ishio, *J. Phys. Soc. Jpn.* **63** (Suppl. A):203 (1994).
20. W. H. Miller, *Adv. Chem. Phys.* **25**:69 (1974); R. A. Jalabert, H. U. Baranger, and A. D. Stone, *Phys. Rev. Lett.* **65**:2442 (1990).
21. K. Nakamura and H. Thomas, *Phys. Rev. Lett.* **61**:247 (1988).